Auto-focusing and self-healing of Pearcey beams

James D. Ring,[1,*] **Jari Lindberg,**[1] **Areti Mourka,**[2] **Michael Mazilu,**[2] **Kishan Dholakia,**[2] **and Mark R. Dennis**[1]

[1]*H H Wills Physics Laboratory, University of Bristol, Tyndall Avenue, Bristol, BS8 1TL, UK*
[2]*SUPA, School of Physics and Astronomy, University of St Andrews, North Haugh, St Andrews, Fife, KY16 9SS, UK*

[*]*james.ring@bristol.ac.uk*

Abstract: We present a new solution of the paraxial equation based on the Pearcey function, which is related to the Airy function and describes diffraction about a cusp caustic. The Pearcey beam displays properties similar not only to Airy beams but also Gaussian and Bessel beams. These properties include an inherent auto-focusing effect, as well as form-invariance on propagation and self-healing. We describe the theory of propagating Pearcey beams and present experimental verification of their auto-focusing and self-healing behaviour.

OCIS codes: (140.3300) Laser beam shaping; (070.2580) Paraxial wave optics; (260.6042) Singular optics.

References and links

1. A. E. Siegman, *Lasers* (University Science Books, 1986).
2. J. Durnin, "Exact solutions for nondiffracting beams. I. The scalar theory," J. Opt. Soc. Am. A **4**, 651–654 (1987).
3. J. Durnin, J. J. Miceli Jr., and J. H. Eberly, "Diffraction-free beams," Phys. Rev. Lett. **58**, 1499–1501 (1987).
4. M. V. Berry and N. L. Balazs, "Nonspreading wave packets," Am. J. Phys. **47**, 264–267 (1979).
5. G. A. Siviloglou and D. N. Christodoulides, "Accelerating finite energy Airy beams," Opt. Lett. **32**, 979–981 (2007).
6. M. A. Bandres and J. C. Gutiérres-Vega, "Ince-Gaussian beams," Opt. Lett. **29**, 144–146 (2004).
7. J. C. Gutiérrez-Vega, M. D. Iturbe-Castillo, and S. Chávez-Cerda, "Alternative formulation for invariant optical fields: Mathieu beams," Opt. Lett. **25**, 1493–1495 (2000).
8. M. A. Bandres, "Accelerating parabolic beams," Opt. Lett. **33**, 1678–1680 (2008).
9. M. V. Berry and C. J. Howls, "Integrals with coalescing saddles," http://dlmf.nist.gov/36.2 (Digital Library of Mathematical Functions, National Institute of Standards and Technology, 2012).
10. T. Poston and I. Stewart, *Catastrophe Theory and its Applications* (Dover Publications Inc., 1997).
11. M. V. Berry and C. Upstill, "Catastrophe optics: morphologies of caustics and their diffraction patterns," Prog. Opt. **18**, 257–346 (1980).
12. G. A. Deschamps, "Gaussian beam as a bundle of complex rays," Electron. Lett. **7**, 684–685 (1971).
13. M. Mazilu, D. J. Stevenson, F. Gunn-Moore, and K. Dholakia, "Light beats the spread: non-diffracting beams," Laser Photon. Rev. **4**, 529–547 (2010).
14. F. O. Fahrbach, P. Simon, and A. Rohrbach, "Microscopy with self-reconstructing beams," Nat. Photon. **4**, 780–785 (2010).
15. Z. Bouchal, J. Wagner, and M. Chlup, "Self-reconstruction of a distorted nondiffracting beam," Opt. Commun. **151**, 207–211 (1998).
16. S. Vyas, Y. Kozawa, and S. Sato, "Self-healing of tightly focused scalar and vector Bessel-Gauss beams at the focal plane," J. Opt. Soc. Am. A **5**, 837–843 (2011).
17. V. Garces-Chavez, D. McGloin, H. Melville, W. Sibbett, and K. Dholakia, "Simultaneous micromanipulation in multiple planes using a self-reconstructing light beam," Nature **419**, 145–147 (2002).
18. P. Vaity and R. P. Singh, "Self-healing property of optical ring lattice," Opt. Lett. **36**, 2994–2996 (2011).
19. F. Gori, G. Guattari, and C. Padovani, "Bessel-Gauss beams," Opt. Commun. **64**, 491–495 (1987).

#170203 - $15.00 USD Received 8 Jun 2012; revised 23 Jul 2012; accepted 23 Jul 2012; published 2 Aug 2012

20. J. E. Morris, M. Mazilu, J. Baumgartl, T. Cizmar, and K. Dholakia, "Propagation characteristics of Airy beams: dependence upon spatial coherence and wavelength," Opt. Express **17**, 13236–13245 (2009).
21. J. Broky, G. A. Siviloglou, A. Dogariu, and D. N. Christodoulides, "Self-healing properties of optical Airy beams," Opt. Express **16**, 12880–12891 (2008).
22. J. Baumgartl, M. Mazilu, and K. Dholakia, "Optically mediated particle clearing using Airy wavepackets," Nat. Photon. **2**, 675–678 (2008).
23. M. V. Berry and C. J. Howls, "Infinity interpreted," Phys. World **6**, 35–39 (1993).
24. J. F. Nye, *Natural Focusing and Fine Structure of Light* (IoP Publishing, 1999).
25. E. Greenfield, M. Segev, W. Walasik, and O. Raz, "Accelerating light beams along arbitrary convex trajectories," Phys. Rev. Lett. **106**, 213902 (2011).
26. T. Pearcey, "The structure of an electromagnetic field in the neighbourhood of a cusp of a caustic," Phil. Mag. S. 7 **37**, 311–317 (1946).
27. M. V. Berry, J. F. Nye, and F. J. Wright, "The elliptic umbilic diffraction catastrophe," Phil. Trans. R. Soc. A **291**, 453–484 (1979).
28. J. J. Stamnes, *Waves in Focal Regions* (Taylor & Francis, 1986).
29. M. A. Bandres and M. Guizar-Sicairos, "Paraxial group," Opt. Lett. **34**, 13–15 (2009).
30. M. Abramowitz and I. A. Stegun, *Handbook of Mathematical Functions* (Dover Publications Inc., 1965).
31. M. V. Berry, "Faster than Fourier," in *Quantum Coherence and Reality*, J. S. Anandan and J. L. Safko, eds. (World Scientific, 1992), 55–65.
32. M. R. Dennis and J. Lindberg "Natural superoscillation of random functions in one and more dimensions," Proc. SPIE **7394**, article 73940A (2009).
33. E. T. F. Rogers, J. Lindberg, T. Roy, S. Savo, J. E. Chad, M R Dennis, and N. I. Zheludev, "A super-oscillatory lens optical microscope for subwavelength imaging," Nature Mat. **11**, 432–435 (2012).
34. J. Baumgartl, S. Kosmeier, M. Mazilu, E. T. F. Rogers, N. I. Zheludev, and K. Dholakia, "Far field subwavelength focusing using optical eigenmodes," Appl. Phy. Lett. **98**, 181109 (2011).
35. M. Anguiano-Morales, A. Martínez, M. D. Iturbe-Castillo, S. Chávez-Cerda, and N. Alcalá-Ochoa, "Self-healing property of a caustic optical beam," Appl. Opt. **46**, 8284–8290 (2007).
36. N. K. Efremidis and D. N. Christodoulides, "Abruptly autofocusing waves," Opt. Lett. **35**, 4045–4047 (2010).
37. D. G. Papazoglou, N. K. Efremidis, D. N. Christodoulides, and S. Tzortzakis, "Observation of abruptly autofocusing waves," Opt. Lett. **36**, 1842–1844 (2011).

1. Introduction

Special functions have in recent years enjoyed a vogue in the classical optics of paraxial beam propagation, owing to their comparative ease of generation, straightforward mathematical representation and, in many cases, structural stability on propagation. Three important examples are the Gaussian beams, [1], Bessel beams [2,3] and Airy beams [4,5]. Many generalizations of these beams have been studied, including, for instance, Hermite-Gaussian, Laguerre-Gaussian and Ince-Gaussian beams [1, 6], Mathieu beams [7], and accelerating parabolic beams [8], all of which exhibit properties characteristic of their respective beam families. Here, we describe a new kind of paraxial beam – the *Pearcey beam* – based on the Pearcey function of catastrophe theory [9,10], which describes diffraction about a cusp caustic and occurs as a two-dimensional counterpart of the Airy function within the catastrophe theory framework [11]. The propagating form of the Pearcey beam has several noteworthy properties, some of which are reminiscent not only of Airy beams, but Gaussian and Bessel beams as well. Most remarkably though, the Pearcey beam possesses an additional auto-focusing property on propagation.

The properties of *Gaussian beams*, as propagating laser cavity modes, are extremely familiar, so some of their striking properties may seem unremarkable. The intensity pattern of a Gaussian beam is invariant upon propagation, apart from an overall transverse scaling. We refer to such beams as *form-invariant*, where the intensity pattern is unchanged up to a similarity transformation (i.e. z-dependent translation, rotation or scaling). Furthermore, starting from the focal plane, a Gaussian beam spreads to its Rayleigh distance z_R, after which the propagation of the field is effectively indistinguishable from that originating from a point source. Mathematically, the Gaussian beam can then be written as the light from this point source translated in the imaginary z-direction [1,12]. The product of the width (second moment) of the Gaussian in the focal plane and in the Fourier plane is the smallest possible for any beam, from the uncertainty prin-

#170203 - $15.00 USD Received 8 Jun 2012; revised 23 Jul 2012; accepted 23 Jul 2012; published 2 Aug 2012

ciple. Thus, a wider range of Fourier components – a greater spectral width – leads to tighter focusing.

Bessel beams are not only form-invariant, but *completely* invariant upon propagation (apart from an overall phase factor), as a result of their Fourier transform being concentrated on a δ-function ring with fixed wavenumber k_r. For this reason, Bessel beams are sometimes described as nondiffracting [2,13] and it is natural to study how the presence of opaque obstacles affect the beam's properties. Indeed, Bessel beams display self-healing over relatively small propagation distances [14–16], making them useful for optical trapping and applications through weakly dispersive media [17]. Laguerre-Gaussian beams also display self-healing, but at much longer distances, comparable to the Rayleigh distance [18]. Since Bessel functions are not strictly normalizable (as their Fourier transforms are δ-concentrated), physical realizations require some modification of a pure Bessel function, achieved by modulating the Bessel function amplitude with a wide Gaussian function in real space, which incurs some diffractive spreading [19].

The profiles of *Airy beams*, similar to Bessel beams, do not change at all on propagation, although the Airy amplitude pattern accelerates in the transverse direction under free-space propagation. These remarkable features have, in recent years, led to intense investigation of Airy beams [4, 5, 20] and their self-healing properties [21, 22]. Physical realizations similarly require modulation of the Airy function, whose total intensity is infinite in the transverse direction.

Historically, Airy functions were introduced by George Biddell Airy [23] to describe the interference fringes sometimes observable below a rainbow, i.e. 'supernumerary rainbows' [24]. They occur more generally as the characteristic diffraction pattern around a caustic of codimension 1 (i.e. a 'fold', which is a line in two dimensions), a fact which has been used to generate beams of cubic and even exponential curvature [25]. Codimension 2 caustics are generically cusps [11], and the characteristic diffraction pattern around them is the so-called Pearcey function [24,26], described below. More complicated caustics occur in three and higher dimensions, classified and understood mathematically via catastrophe theory [10] including their topologies and characteristic diffraction patterns [11, 24, 27].

The properties of paraxially propagating Airy beams do not seem directly related to their connection with diffraction catastrophes, beyond the observation that caustics, like propagating Airy beams, are curved [11]. It is therefore natural to ask whether the next member of the catastrophe optics hierarchy, the Pearcey function, has unusual propagation properties. We investigate such a beam here, and show, in addition to its self-healing and form-invariance upon propagation, the Pearcey beam auto-focuses in a remarkable way at a propagation distance mathematically analogous to the Rayleigh distance of a Gaussian beam, and the pattern spatially inverts beyond this focus. Like the Bessel beam and Airy beam, a pure Pearcey beam has infinite energy, but can be made finite by modulating the Pearcey function with a Gaussian in real space, which does not significantly change the beam's properties. We formulate the Pearcey beam analytically and present experimental results of the finite energy Pearcey-Gauss beam generation using computer-controlled holograms, corroborating the properties we describe.

In catastrophe optics, the Pearcey function represents the diffraction about a focus in $1+1$ dimensions, which experiences spherical aberration – the rays underlying the diffraction caustic form a cusp either below or above the geometrical focus depending on the sign of the spherical aberration. In a sense, the propagating Pearcey beam simulates such a $1+1$ dimensional aberrated focus in each transverse plane, with different amounts of aberration (positive or negative) for different z. This picture accounts for the form-invariance of the Pearcey beam, since each different amount of aberration gives a differently-scaled Pearcey function, and the autofocusing plane is the plane in which the aberration is zero, i.e. it looks like the 1+1 propagation

#170203 - $15.00 USD Received 8 Jun 2012; revised 23 Jul 2012; accepted 23 Jul 2012; published 2 Aug 2012

pattern of a focused beam. The beam inversion occurs beyond this distance when the aberration has changed sign.

The structure of this paper is as follows. In section 2 we mathematically construct the analytic form of the paraxially propagating Pearcey beam and the more physical Pearcey-Gauss beam, describing their auto-focusing and associated inversion. In section 3 we investigate the nature of the focal spot formed by the finite energy Pearcey-Gauss beam and in section 4 we present experimental results, demonstrating the beam's auto-focusing and self-healing properties. We conclude in section 5 with further discussion and outlook.

2. The Pearcey beam

The Pearcey function is defined [9, 26] by an integral representation,

$$\mathrm{Pe}(X,Y) \equiv \int_{-\infty}^{\infty} \mathrm{d}s \, \exp\left[\mathrm{i}\left(s^4 + s^2 Y + sX\right)\right], \tag{1}$$

where X and Y are dimensionless variables transverse to propagation in the z-direction. In real space, the Pearcey function is $\mathrm{Pe}(x/x_0, y/y_0)$, with x_0, y_0 specified scaling lengths. The intensity pattern of $\mathrm{Pe}(x/x_0, y/y_0)$ is shown in Fig. 1(a) for $x_0 = y_0 = 0.1$ mm, along with the cusp caustic which underlies the amplitude pattern. Equation (1) can be calculated numerically using a contour rotation in the complex s plane, $s \to s' \mathrm{e}^{\mathrm{i}\pi/8}$, which guarantees convergence of the integral as $s' \to \pm\infty$. The mathematical definition of the Airy function is similar; the quartic polynomial exponent in Eq. (1) is replaced by a cubic $s^3 + sx/x_0$, which has a fold singularity at the origin, separating a two-wave interference pattern from an exponentially decaying region with no waves [28].

The form of the cusp which underpins the intensity pattern can be expressed [28] as the (x,y) points satisfying

$$\left(\frac{2y}{3y_0}\right)^3 + \left(\frac{x}{x_0}\right)^2 = 0. \tag{2}$$

The two-dimensional curve parameterised by this expression is shown as a white dashed line in Fig. 1(a). The values of x_0 and y_0 determine the cartesian scalings of the cusp, which itself is important in the anatomy of the Pearcey function; the line demarcates two interference regimes in the pattern, corresponding to a single wave and three wave interference. The Pearcey function of Eq. (1) can be understood mathematically by the contributing saddle points from the integral in the complex s-plane. The cusp is then the locus of coalescence of these saddle points, but in this case the saddles do not correspond directly to optical rays, which is different from the occurrence of a cusp in geometric catastrophe optics [11, 24].

The Fourier transform of the Pearcey function can be expressed as

$$\begin{aligned}\widetilde{\mathrm{Pe}}(k_x x_0, k_y y_0) &= \frac{1}{(2\pi)^2} \int_{-\infty}^{\infty}\int_{-\infty}^{\infty} \mathrm{d}x\mathrm{d}y \, \mathrm{Pe}\left(\frac{x}{x_0}, \frac{y}{y_0}\right) \mathrm{e}^{-\mathrm{i}k_x x - \mathrm{i}k_y y} \\ &= x_0 y_0 \, \mathrm{e}^{\mathrm{i}k_x^4 x_0^4} \delta\left(k_x^2 x_0^2 - k_y y_0\right),\end{aligned} \tag{3}$$

where k_x and k_y are the Fourier pairs of x and y respectively, and δ denotes the Dirac delta-function. Equation (3) thus describes a δ-line concentrated on the parabola $k_x^2 x_0^2 = k_y y_0$, modulated by a k_x-dependent phase factor. Despite having real-space representations closely related by catastrophe optics, the Fourier transforms of the Pearcey and Airy functions differ - the latter has a uniform amplitude and cubic phase dependence. The concentration on a curve in Fourier space is more reminiscent of the Fourier representation of a Bessel beam, although the

#170203 - $15.00 USD Received 8 Jun 2012; revised 23 Jul 2012; accepted 23 Jul 2012; published 2 Aug 2012

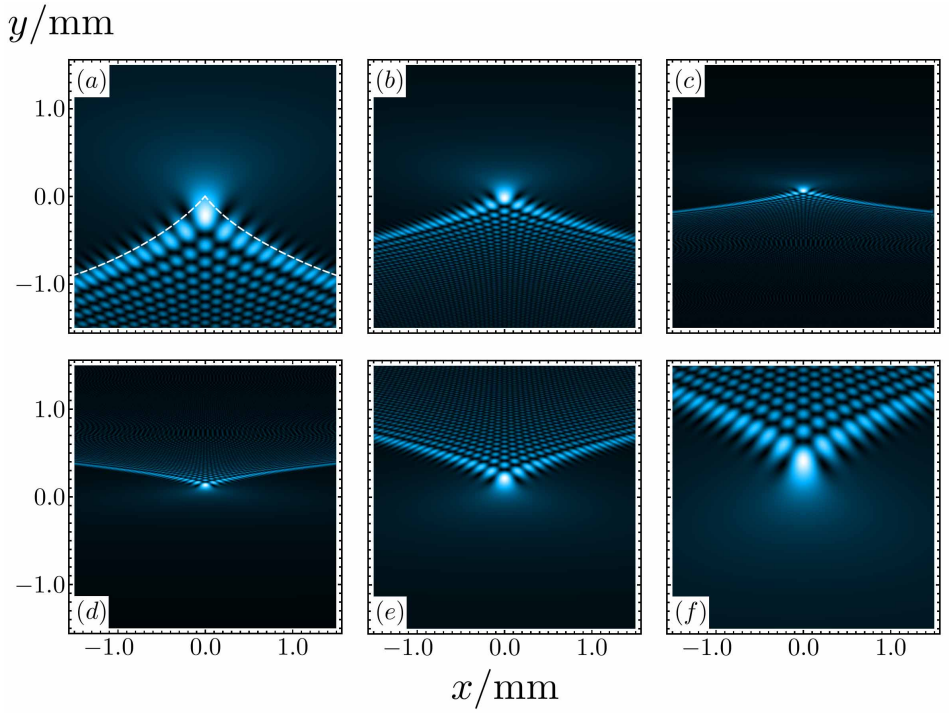

Fig. 1. Transverse profile intensities of the Pearcey beam, with parameters $x_0 = y_0 = 10^{-4}$ m and where $z_e \equiv 2ky_0^2 \approx 0.251$ m and k is the wavenumber for wavelength $\lambda = 500$ nm; (a) intensity of the Pearcey function for $z = 0$ m; (b) the Pearcey beam at $z = 0.8z_e$ m; (c) at $z = 0.975z_e$ m; (d) at $z = 1.025z_e$ m; (e) $z = 1.2z_e$ m; (f) $z = 2z_e$ m. The cusp underlying the Pearcey pattern is shown as a white dashed line in (a). Upon propagation, the cusp - and therefore the shape of the Pearcey pattern - flattens out to a line, then inverts after a singular plane at $z = z_e$.

magnitude of the Pearcey wave vectors is not fixed (and hence the beam profile changes on propagation).

An analytic form of the propagating monochromatic Pearcey beam can be found using the paraxial, scalar Huygens-Fresnel integral [1] for an initial field (at $z = 0$) given by the Pearcey function Eq. (1). This takes the form

$$\begin{aligned} \mathrm{Pe}_{\mathrm{beam}}(x,y,z) &= \frac{-\mathrm{i}k}{2\pi z}\int_{-\infty}^{\infty}\int_{-\infty}^{\infty}\mathrm{d}x'\mathrm{d}y'\ \mathrm{Pe}\left(\frac{x'}{x_0},\frac{y'}{y_0}\right)\exp\left(\frac{\mathrm{i}k}{2z}\left[(x-x')^2+(y-y')^2\right]\right) \\ &= \frac{1}{(1-z/z_e)^{\frac{1}{4}}}\mathrm{Pe}\left(\frac{x}{x_0(1-z/z_e)^{\frac{1}{4}}},\frac{y-zy_0/2kx_0^2}{y_0(1-z/z_e)^{\frac{1}{2}}}\right), \end{aligned} \tag{4}$$

where k is the wavenumber and we define $z_e \equiv 2ky_0^2$. This expression reveals how naturally the Pearcey function propagates paraxially: it retains its form as a Pearcey function as z evolves, although the scalings in x and y are different, making the shape of the underlying cusp z-dependent. Furthermore, as z increases the Pearcey pattern is translated linearly in y, unlike an Airy beam whose transverse translation depends quadratically on z. Equation (4) and Eq. (2)

#170203 - $15.00 USD Received 8 Jun 2012; revised 23 Jul 2012; accepted 23 Jul 2012; published 2 Aug 2012

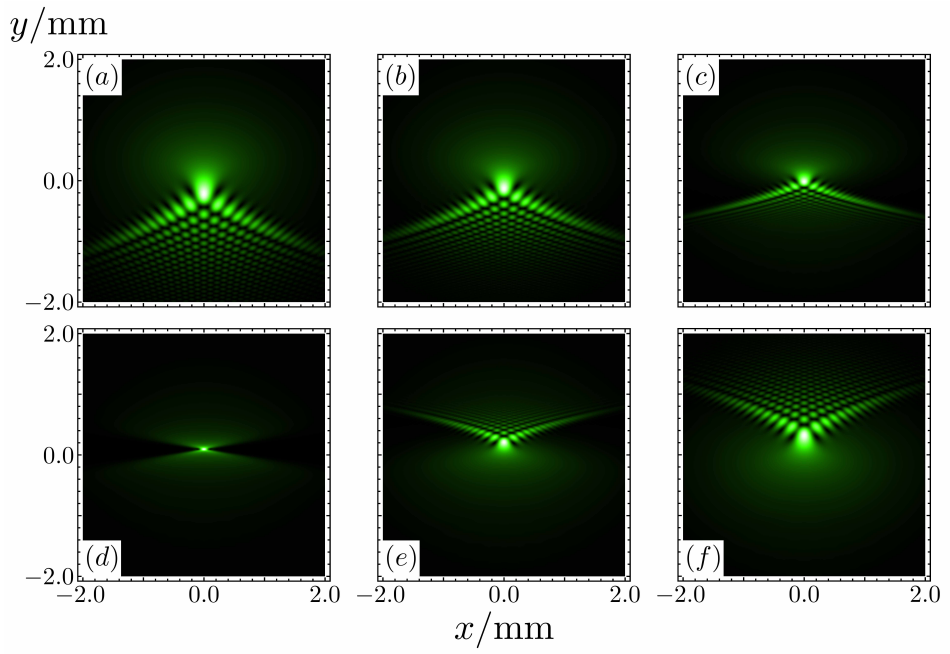

Fig. 2. Transverse intensity of a Pearcey-Gauss beam as z increases for $x_0 = y_0 = 0.1$ mm, $w_0 = 2.0$ mm and $\lambda = 500$ nm. The scaling and inversion of the pattern is still evident, however, there now exists a small hourglass-shaped focal point that was absent in case of the unmodulated Pearcey beam. The intensities of each image are not on the same scale.

may be combined to give an expression for the evolution of the cusp in z,

$$\left(\frac{2}{3}\frac{y - zy_0/2kx_0^2}{y_0\left(1-z/z_e\right)^{\frac{1}{2}}}\right)^3 + \left(\frac{x}{x_0\left(1-z/z_e\right)^{\frac{1}{4}}}\right)^2 = 0. \tag{5}$$

Figures 1(a)–1(f) show the intensity pattern of the Pearcey beam as z increases. The rate of scaling becomes infinitely fast as z approaches z_e but changes more quickly in the y-direction than in x. As a result, the bright fold catastrophe 'arms' of the Pearcey pattern appear to lift upwards towards the line $y = y_0^3/x_0^2$, and the intensity becomes more concentrated as $z \to z_e$. We see from Eq. (4) that this occurs because there is a singularity in both x and y at $z = z_e$, so the scaling is effectively infinite (which is possible since the total Pearcey pattern cannot be normalized). When $z > z_e$, Eq. (5) has a real solution with an inverted cusp mirroring the behavior of the cusp when $z < z_e$, and the Pearcey function follows the inversion of the cusp, as evident from Fig. 1; this spatial inversion is of course expected for a light beam passing through a focus. In the 'focusing' plane the beam is singular, taking the form

$$\mathrm{Pe}_{\mathrm{beam}}(x,y,z_e) = e^{i\pi/4}\sqrt{\frac{\pi}{y/y_0 - y_0^2/x_0^2}}\exp\left(\frac{-ix^2y_0}{4\left(yx_0^2 - y_0^3\right)}\right). \tag{6}$$

This is an infinitely bright line (with varying phase) parallel to the x-axis at $y = y_0^3/x_0^2$.

The singularity can be understood mathematically using a complex analysis approach. When x_0 and y_0 are replaced with the z-dependent scalings from Eq. (4), the Pearcey integrand of Eq. (1) can be considered as a complex function of z. This function has an *essential singularity*

#170203 - $15.00 USD Received 8 Jun 2012; revised 23 Jul 2012; accepted 23 Jul 2012; published 2 Aug 2012

at $z = z_e$, i.e. a reciprocal-type singularity in the exponent, which is real-valued, accompanied by a branch point singularity multiplying the exponential. This contrasts with the propagating form of a Gaussian beam

$$\mathrm{G}(x,y,z) = \frac{1}{(1+\mathrm{i}z/z_\mathrm{R})}\exp\left(-\frac{x^2+y^2}{w_0^2(1+\mathrm{i}z/z_\mathrm{R})}\right), \tag{7}$$

where $z_\mathrm{R} = kw_0^2/2$ is the Rayleigh distance and w_0 is the width of the beam at the beam waist ($z = 0$).

In the Gaussian beam, there is an essential singularity at $\mathrm{i}z_\mathrm{R}$, interpreted physically as a 'complex source' [1, 12]. In this interpretation, the Gaussian waist corresponds to the best possible image of this complex point source, achieved when it is closest to the real z-axis. The Pearcey beam integrand, on the other hand, has its singularity on the real line, and effectively passes through it upon propagation. The form of the singularity is more complicated in the Pearcey beam case, and the corresponding pattern in the singular plane $z = z_e$ is completely delocalized in x. Therefore, the limits imposed on the transverse scalings in the Gaussian case do not apply for the Pearcey beam and we see from Eq. (4) that as $z \to z_e$ the factors scaling x and y tend to infinity, highly concentrating the intensity of the beam to a line in this particular z-plane. We refer to this phenomenon as *essential focusing* – a high concentration of intensity due to the existence of a real-valued essential singularity in the z-dependence. In a sense, this is analogous to limiting the waist width and hence the Rayleigh distance of a Gaussian beam to zero, making the Gaussian's 'complex source' real-valued and the beam infinitely localized in the waist plane. Therefore, the bright line from the real essential singularity (described by Eq. (6)) is, in a sense, a 'source' for the propagating Pearcey pattern.

Of course, the Pearcey beam's essential singularity is not physical. For the paraxial approximation to be valid it is necessary that the transverse spatial spectrum is small so that $|k_x|, |k_y| \ll k$, but from Eq. (3) it is evident that such limitations do not exist for the Pearcey beam, giving rise to the observed singular behaviour. Fortunately, as with the Airy beam, the rapidly oscillating phases at large k_x and k_y do not contribute due to cancellation, and it is possible to experimentally realise an approximation of the Pearcey beam from the spectrum near the origin. A natural regularization is to modulate the initial Pearcey pattern by a Gaussian with large width w_0, which gives the Pearcey pattern finite total intensity whilst maintaining its analytic tractability and limiting its spectrum. In Eq. (4), it is easy to include a Gaussian $\exp(-(x^2+y^2)/w_0^2)$ in the intensity profile and integrate as before (or alternatively via the ABCD approach of Ref. [29]). Therefore the propagating form of this finite energy Pearcey-Gauss beam is

$$\mathrm{PeG}(x,y,z) = \frac{\mathrm{G}(x,y,z)}{[1-z/\zeta(z)z_\mathrm{e}]^{\frac{1}{4}}}\mathrm{Pe}\left(\frac{x}{x_0\zeta(z)[1-z/\zeta(z)z_\mathrm{e}]^{\frac{1}{4}}}, \frac{y-zy_0/2kx_0^2}{y_0\zeta(z)[1-z/\zeta(z)z_\mathrm{e}]^{\frac{1}{2}}}\right), \tag{8}$$

where $\zeta(z) = (1+\mathrm{i}z/z_\mathrm{R})$ and $\mathrm{G}(x,y,z)$ is defined in Eq. (7). As with many analytic forms of beams made from modulating a function by a Gaussian, the Pearcey-Gauss beam has a complex argument upon propagation in z, giving rise to the complex analytic continuation of the Pearcey function, which maintains a form very similar to a Pearcey function with real arguments.

Figure 2 shows the Pearcey-Gauss intensity pattern from Eq. (8). Evidently, the Gaussian modulation does not affect the main behavior of the Pearcey beam – the same arm-straightening, auto-focusing and inversion effects are evident as for the Pearcey beam of Eq. (4). However, in the modulated case, the additional imaginary part of $\zeta(z)$ in Eq. (8) gives the problematic essential singularity a very small imaginary part. The increase of the x and y scalings still occurs, as does the inversion, but now with finite intensity across the beam and a slight deformation

#170203 - $15.00 USD Received 8 Jun 2012; revised 23 Jul 2012; accepted 23 Jul 2012; published 2 Aug 2012

to the original Pearcey function with real arguments. In the new essential focusing plane, the infinite line becomes a small spot centred in an hourglass-shaped profile as depicted in Fig. 2(d). That is, modulation with a Gaussian has made the essential singularity 'source' complex, but in this case it is closer than one Rayleigh distance to the real z-axis. The result is a small anisotropic spot of high intensity, shown in Fig. 2(d).

The Fourier transform of the Pearcey-Gauss beam can be calculated by convolving Eq. (3) with the Fourier transform of the modulating Gaussian, according to the convolution theorem. This gives the expression

$$\widetilde{\mathrm{PeG}}(k_x,k_y)=\frac{w^2\exp\left[-w^2\left(k_x^2+k_y^2\right)/4\right]}{4\pi\left(1+\mathrm{i}w^2/4y_0^2\right)^{1/4}}\mathrm{Pe}\left(\frac{w^2k_x}{2\mathrm{i}x_0\left(1+\mathrm{i}w^2/4y_0^2\right)^{1/4}},\frac{w^2(k_y-y_0/2x_0^2)}{2\mathrm{i}y_0\left(1+\mathrm{i}w^2/4y_0^2\right)^{1/2}}\right), \tag{9}$$

where k_x and k_y are the Fourier pairs of x and y. In general, the centre of this Fourier distribution has a positive k_y value (accounting for the upwards motion of the Pearcey beam on propagation) and mimics the shape of the δ-line parabola of Eq. (3), despite the fact it can be expressed as a Pearcey function. Figure 3(b) shows the intensity of Eq. (9) for the parameters of Fig. 2 ($x_0=y_0=0.1$ mm, $w_0=2.0$ mm and $\lambda=500$ nm).

3. The Pearcey-Gauss focus

In the introduction, we proposed the interpretation that each two-dimensional transverse plane of the Pearcey beam can be imagined as a 'simulation' of a spherically aberrated one-dimensional wavepacket in x, being focused as it 'propagates' in y. That is, the transverse plane of the beam *appears* to be a longitudinal section of a spherically aberrated focus. The amount of aberration depends on z, and in the essential focusing plane ($z=z_\mathrm{e}$) the beam simulates the pattern around a point focus with *zero* aberration. This explains the 'hourglass' shape of the intensity distribution in Fig. 2(d). As w_0 (the width of the modulating Gaussian in Eq. (8)) increases, the Pearcey-Gauss beam becomes more like the infinite-energy Pearcey beam and – in the limit of infinite w_0 – the essential focusing plane becomes a section of a focus of unit numerical aperture (assuming a refractive index of 1). However, before this limit is reached, the essential focus has an intensity peak with a narrow FWHM in both the x- and y-directions.

Closed form expressions for the shape of the essential focus along the x- and y-directions are in fact possible and respectively take the form

$$\mathrm{PeG}(x,y_0^3/x_0^2,z_\mathrm{e})=\exp\left(\frac{-x^2-y_0^6/x_0^4}{w_0^2\zeta(z_\mathrm{e})}\right)\sqrt{\frac{w_0}{2y_0\zeta(z_\mathrm{e})^{3/2}}}\left[2\Gamma\left(\frac{5}{4}\right)\,{}_0F_2\left(;\frac{1}{2},\frac{3}{4};\frac{w_0^2x^4}{2^{10}\zeta(z_\mathrm{e})^3x_0^4y_0^2}\right)\right.$$
$$\left.+\frac{w_0x^2}{2^5\zeta(z_\mathrm{e})^{3/2}y_0x_0^2}\Gamma\left(-\frac{1}{4}\right)\,{}_0F_2\left(;\frac{5}{4},\frac{3}{2};\frac{w_0^2x^4}{2^{10}\zeta(z_\mathrm{e})^3x_0^4y_0^2}\right)\right], \tag{10}$$

and

$$\mathrm{PeG}(0,y,z_\mathrm{e})=\exp\left(\frac{-y^2}{w_0^2\zeta(z_\mathrm{e})}\right)\frac{\mathrm{e}^{-\mathrm{i}\pi/4}w_0}{4\zeta(z_\mathrm{e})y_0}\sqrt{\frac{y}{y_0}-\frac{y_0^2}{x_0^2}}\exp\left[-\frac{w_0^2}{32\zeta(z_\mathrm{e})}\left(\frac{y}{y_0^2}-\frac{y_0}{x_0^2}\right)^2\right]$$
$$\times K_{\frac{1}{4}}\left[-\frac{w_0^2}{32\zeta(z_\mathrm{e})}\left(\frac{y}{y_0^2}-\frac{y_0}{x_0^2}\right)^2\right], \tag{11}$$

where Γ is the gamma function, ${}_0F_2$ is a generalized hypergeometric function and $K_{1/4}$ is a quarter order modified Bessel function of the second kind [30].

#170203 - $15.00 USD Received 8 Jun 2012; revised 23 Jul 2012; accepted 23 Jul 2012; published 2 Aug 2012

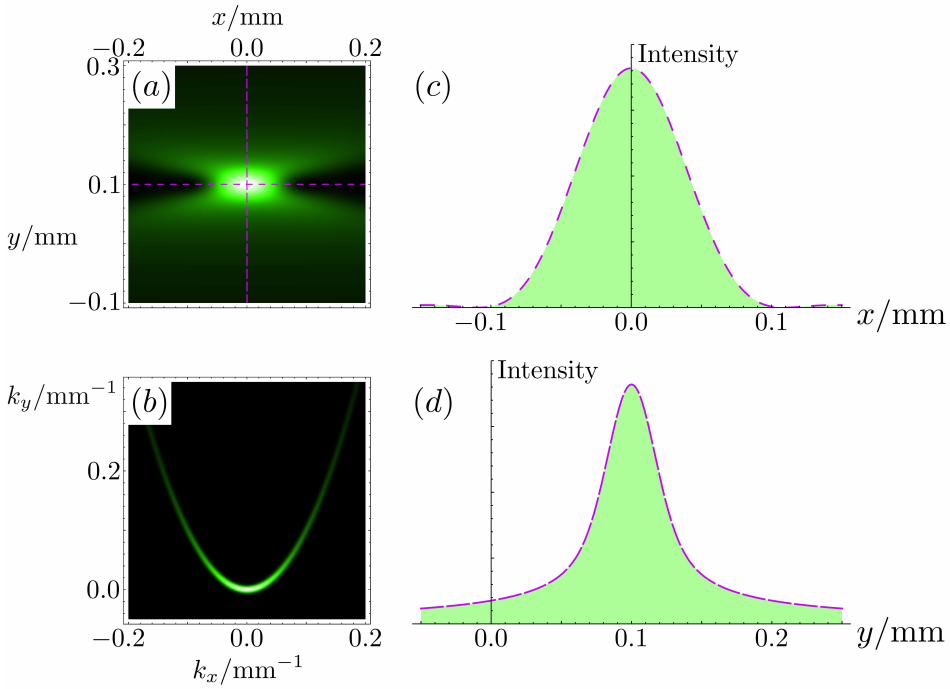

Fig. 3. Intensity of the Pearcey-Gauss beam (for $x_0 = y_0 = 0.1$ mm, $w_0 = 2.0$ mm and $\lambda = 500$ nm) at the essential focusing plane; (a) magnification of the essential focus of Fig. 2; the dashed lines correspond to the intensity cross-sections of (c) and (d); (b) intensity of the Fourier distribution of the Pearcey-Gauss beam according to Eq. (9), which mimics the δ-line parabola of Eq. (3); (c) the short-dashed line shows the intensity cross-section of the essential focus in the x-direction; (d) intensity cross-section along the long-dashed line of (a) in the y-direction.

Figure 3(a) shows a magnification of the essential focus of the Pearcey-Gauss beam – Eq. (8) for $z = z_e$. Figures 3(c) and 3(d) show the intensity cross-sections of the essential focus given by Eqs. (10) and (11) respectively. The width of the essential focus in the x- and y-directions is not significantly smaller than that of an astigmatic Gaussian of equal spectral width.

We note here that the dark regions in the neck of the hourglass display significant super-oscillatory behaviour [31], in keeping with the understanding that narrow focal spots are often bounded by highly super-oscillatory regions [32–34].

4. Experimental realization of the Pearcey beam

Our experimental realization of a Pearcey beam (or, more accurately, a Pearcey-Gauss beam) involved encoding a Pearcey-Gauss spectrum (as in Eq. (9)) onto a spatial light modulator (SLM). The image encoded onto the SLM is shown in Fig. 4(b), and was incorporated into the experimental set up as described in Fig. 4(a). A helium-neon laser source ($\lambda = 633$nm, $P_{\max} = 5$mW) was used and the beam was sent through a 50μm pinhole in order to obtain an initially homogeneous Gaussian intensity profile. The beam was then expanded with a telescope (L_1 and L_2) in order to slightly overfill the SLM (a Holoeye LC-R 2500). The SLM operated in the standard first-order diffraction configuration and the Pearcey beam was created in the far-field of the SLM. In order to filter the first order beam carrying the Pearcey pattern from the unmodulated zero-order beam, a pinhole aperture was located in the back focal plane of lens

#170203 - $15.00 USD Received 8 Jun 2012; revised 23 Jul 2012; accepted 23 Jul 2012; published 2 Aug 2012

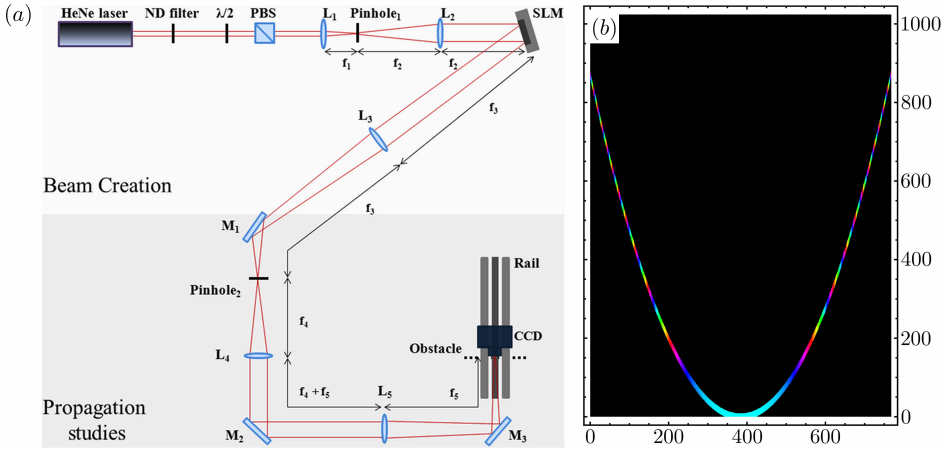

Fig. 4. Experimental setup; (a) schematic of the experiment, where L_i are lenses, SLM is the spatial light modulator, CCD is the charge coupled device camera, PBS is a polarizing beam splitter; the focal widths of lenses are $f_1 = 25$ mm, $f_2 = 100$ cm, $f_3 = 680$ mm, $f_4 = 400$ mm and $f_5 = 800$ mm; (b) image encoded on the SLM. The Fourier transform of the Pearcey-Gauss beam describes a parabola with phase given by Eq. (9). The hue indicates the phase while brightness describes the corresponding intensity. The SLM was used in the standard first-order diffraction configuration.

L_3. To study the consecutive transverse cross-sections of the resulting Pearcey beam, another telescope (lenses L_4 and L_5) was used to image it on the obstacle and subsequently on a CCD camera (Basler piA640-210gm, pixel size: 7.4μm $\times$ 7.4μm), in order to record the images. The CCD camera was in the Fourier plane of the SLM and was mounted on a translation stage in order to get images over the propagation range of the beam.

Figure 5 shows the experimentally obtained images for the propagation distances indicated. These results support the theoretical predictions, exhibiting inversion as well as auto-focusing at the essential focus plane. We note that the precise position of the focus is dependent on the experimental setup. Figure 5(d) shows the essential focus, which is similar to that shown in Fig. 2(d).

We also demonstrated experimentally the capability of the Pearcey beam to self-heal. Figure 6 shows the experimental results of applying a rectangular obstacle (indicated by the white line in Fig. 6(a)) to the $z = 0$ plane of the Pearcey-Gauss beam. These results clearly display a revival of the Pearcey pattern after the essential focusing, which is still strongly evident in the propagation of the beam. Numerical results for small perturbations to the Pearcey-Gauss beam display pattern revival after a distance of as little as 5 cm. Larger perturbations cause a greater disturbance and recovery of the beam profile requires propagation over a longer distance; for example, blocking the main intensity lobe of the beam revives after a propagation distance of the order of 20 cm. These lengths are similar to those of an Airy beam for comparable parameters and obstructions [21]. Significantly, the Pearcey-Gauss beam's profile recovers close to its original form after the inversion for all but the most severe disturbances. We conclude that, similar to Airy and Bessel beams, small perturbations to the field of the Pearcey beam do not drastically effect the intensity pattern at greater propagation distances, especially not after the inversion plane.

It is not clear how to define the concept of self-healing rigorously, although it is clear conceptually. A detailed study of self-healing is outside the scope of the present paper, but we

#170203 - $15.00 USD Received 8 Jun 2012; revised 23 Jul 2012; accepted 23 Jul 2012; published 2 Aug 2012

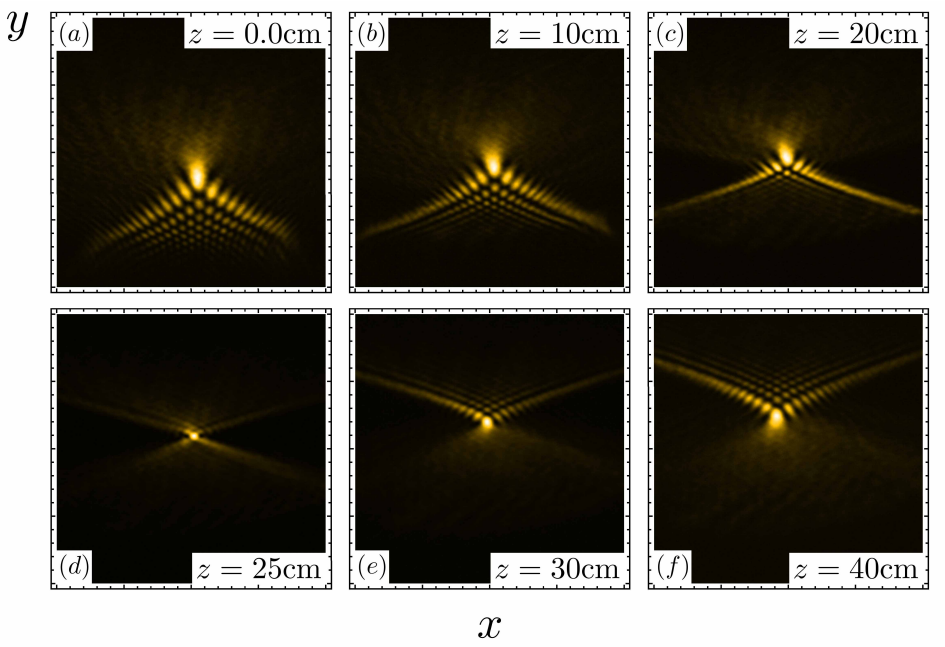

Fig. 5. Experimental observation of the Pearcey-Gauss beam for consecutive propagation distances. The collapse of the beam to a point is clearly visible, as well as the predicted inversion. These results agree with the theoretical and numerical predictions. The propagation distances are given, inset in the images.

note that since the Pearcey beam is *not* nondiffracting and *is* self-healing, there is compelling reason to decouple these two concepts – self-healing beams are not, by necessity, nondiffracting (although the opposite may be typical) [18, 35]. This is particularly striking in the case of the Pearcey beam, as its cross-section consists of a complicated interference pattern, which is robust – apart from rescaling – both to propagation and disruption by small obstacles.

5. Discussion

We have introduced a new beam profile based on the Pearcey function of catastrophe optics. Its transverse profile looks like a diffraction cusp, which, upon propagation, auto-focuses to a small spot centred in an hourglass-shaped intensity distribution. The beam profile then spatially inverts after this plane.

Our analysis has highlighted similarities of this propagation to three well-known beams of paraxial optics: Gaussian, Bessel and Airy beams. The definition of the Pearcey function and its relation to caustics is similar to the Airy function, and, like a Gaussian, it is form-invariant with a focus given by an essential singularity (which is real for a Pearcey beam, and imaginary for a Gaussian). Also, the Pearcey beam's spatial spectrum is concentrated on a δ-parabola, similar to the δ-ring of a Bessel beam's Fourier transform. Simple superpositions of Pearcey beams would therefore be easily possible because of the small bright area required on an SLM to form them. The Pearcey beam also exhibits self-healing properties analogously to Airy and Bessel beams, making it robust to local obstructions and potentially useful for cell or micro-particle manipulation but notably is not propagation invariant (non-diffracting).

The essential focusing exhibited by the Pearcey beam is a generalization of the complex source approach to Gaussian beams, with an integral representation whose integrand has a real-

#170203 - $15.00 USD Received 8 Jun 2012; revised 23 Jul 2012; accepted 23 Jul 2012; published 2 Aug 2012

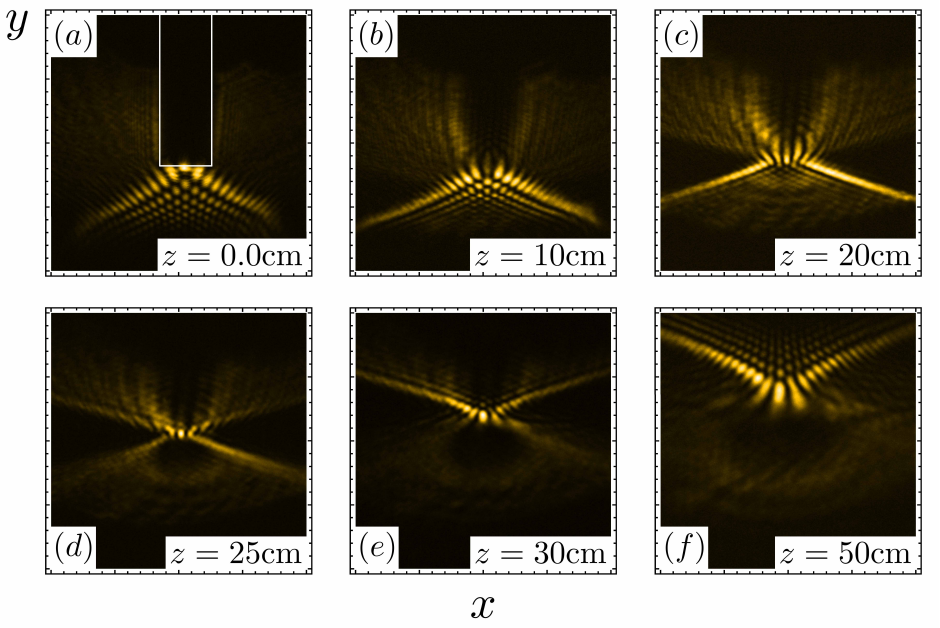

Fig. 6. Experimental images of the self-healing of the Pearcey beam from an arbitrary perturbation. The obstacle was cylindrical, with a rectangular projection, and the area blocked is indicated by the white line in (a). It is clear that the Pearcey beam recovers from the initial perturbation and still collapses and inverts after its essential focus.

valued 'source', giving rise to a singular focusing plane. We note that although essential focusing is superficially similar to abrupt autofocusing [36,37], they are mathematically distinct. We also note that there is some similarity to the so-called 'caustic beam' [35], which appears to be based on an astroid of four cusps, but which does not display any auto-focusing.

Mathematically, the essential focusing we have described for Pearcey beams will occur for any transverse amplitude distribution given by a function of the form

$$U(x,y) = \int_{-\infty}^{\infty} \mathrm{d}s \, \exp\left[\mathrm{i}\left(s^{2n} + ys^{n} + xs^{m}\right)\right], \tag{12}$$

where n and m are integers such that $n > m$. Beams of this description are form invariant on propagation for all $n = 2m$, but it is not apparent that any such generalization would have a distinct advantage over the Pearcey function with regards to the properties discussed in this paper. We anticipate, however, that there are further profiles inspired by special functions, which propagate to singularities on the real axis. It is likely these will also have interesting focusing properties.

Acknowledgments

We are grateful for discussions with John Hannay, Jörg Götte, Anna Khoroshun and Stefan Skupin. We gratefully acknowledge funding from the EPSRC. KD is a Royal Society Wolfson Merit Award holder and MRD is a Royal Society University Research Fellow.

#170203 - $15.00 USD Received 8 Jun 2012; revised 23 Jul 2012; accepted 23 Jul 2012; published 2 Aug 2012